Phase transitions in systems with extremely short-ranged attractions: A density-functional theory

C. Rascón and G. Navascués
Departamento de Física de la Materia Condensada, Universidad Autónoma, Cantoblanco, Madrid E-28049, Spain and Instituto de Ciencia de Materiales (Consejo Superior de Investigaciones Científicas), Cantoblanco, Madrid E-28049, Spain

L. Mederos
Instituto de Ciencia de Materiales (Consejo Superior de Investigaciones Científicas), Cantoblanco, Madrid E-28049, Spain
(Received 7 November 1994; revised manuscript received 16 January 1995)

We obtain the phase diagram of a classical simple system of interacting particles. We use the square-well model potential to study the effect of extremely short-ranged attractive interactions on the phase diagram. In particular, we focus the attention on the solid-solid transition recently reported in the literature [Bolhuis *et al.*, Phys. Rev. Lett. **72**, 2211 (1994)]. We use a functional-perturbation approximation for the free energy. The theory predicts a first-order transition between two solid phases with the same structure, in agreement with recent Monte Carlo simulations. A discussion about the mechanism responsible for this transition is also included.

I. INTRODUCTION

The pair potential describing the interaction between two particles in a classical simple system, like a rare gas, consists of two parts: an attractive tail over large distances (large compared with the particle size) and a repulsive core at short ones. It is known that these two contributions play different roles when determining the phase diagram of the system. The attraction between particles is responsible for the gas condensation into a liquid phase. On the other hand, the fluid freezing into a solid phase can be essentially understood in terms of the packing properties which are controlled by the short-ranged repulsion. Then, the attraction determines somehow the relative stability of the liquid phase with respect to the other phases (gas and solid) present in the phase diagram. Moreover, when the range of the attractive interaction is small enough, it is expected that the liquid phase will be absent from the phase diagram. This is because before a van der Waals loop is generated, as the gas density increases, the system can reduce its free energy, transforming itself into a solid. There is not much evidence of this behavior for simple systems because of the relatively large range of the attractive interaction of most of the intermolecular potentials. A possible exception, recently reported,[1–3] is the high-temperature phase diagram of the fullerene C_{60}. For high enough temperatures (above room temperature) C_{60} behaves as a simple system.[4] Under these conditions the interaction between two C_{60} molecules can be reasonably approximated by the central Girifalco potential.[4] When this potential is compared with the standard Lennard-Jones (LJ) potential (which very accurately matches the interaction between two rare gas atoms) of the same well depth, a main difference becomes apparent. The attractive tail of the Girifalco potential goes to zero significantly faster than the LJ one does. There is a rough way to estimate the effect of this difference on the phase diagram and, in particular, on the stability of the liquid phase of C_{60}. The main qualitative effect will be a reduction of the critical point temperature T_c (measured in units of the well depth) while the triple-point temperature T_t can be expected to be also lowered but in a significantly much smaller amount. If the reduction in T_c is large enough, we will have a phase diagram where the sublimation line is always above the liquid-gas coexistence curve. Therefore, the liquid phase will be absent from the phase diagram. On the other hand, the ratio between the attraction and the hard core free energy (proportional to the molecular size) controls, in some sense, the position of the critical point relative to the triple point. So we compare the ratio

$$\frac{4\pi \int_\sigma^\infty dr r^2 \frac{\varphi_{att}(r)}{\epsilon}}{\frac{4\pi}{3}\sigma^3}, \tag{1}$$

where ϵ is the potential well depth and σ is defined by $\varphi(r=\sigma)=0$, for both the LJ and the Girifalco potentials. When this is done, we find that the ratio (1) for the LJ potential is 3 times larger than the corresponding result for the Girifalco potential. If this is combined with the fact that $\frac{T_c}{T_t} \approx 2$ for the LJ potential,[3] we conclude that it is reasonable to expect that the Girifalco potential will possibly give a phase diagram where the liquid phase is not stable. Molecular dynamics (MD) simulations[1] and Gibbs ensemble Monte Carlo (MC) simulations[2] as well as theoretical results[1,3] have been recently presented for the Girifalco potential. Although the MD results support the existence of a stable liquid phase in a narrow range of temperatures, the MC simulations give a phase diagram without liquid phase. The theoretical results seem to support the MD ones but, after a careful analysis,[3] they could even agree with the MC results. In summary,

the Girifalco potential is quite close to the critical interaction potential which precludes the existence of the liquid phase.

Experimental evidence of this behavior exists for a different kind of systems, namely, in mixtures of colloidal particles with polymers.[5,6] The presence of the polymer can be taken into account through an effective attractive interaction between the colloidal particles whose range is related to the polymer size.[7,8] This gives the chance for producing real *simple* systems with extreme pair potentials and, in particular, with very short-ranged attractive interactions. Some computer simulation[9] and theoretical[10] efforts have been recently dedicated to study the phase diagram (including the solid phase) of simple systems with varying range of their attractive interactions. The expected behavior has been found and, in particular, the theory predicts a value for the range of the attractive tail where the liquid phase disappears which is in reasonably good agreement with the simulation result. However, an unexpected new transition has been recently reported by Bolhuis and Frenkel.[11] These authors, using Monte Carlo simulations, have found that, if the range of the attractive forces is short enough, a solid-solid transition emerges in the phase diagram. The effective simple interaction between colloidal particles has been modeled through the square-well potential:

$$\varphi(r) = \begin{cases} \infty & , \quad r < \sigma, \\ -\epsilon & , \quad \sigma \leq r < \sigma + \delta, \\ 0 & , \quad r \geq \sigma + \delta, \end{cases} \tag{2}$$

where σ is the diameter of the colloidal particle and ϵ and δ are the depth and width of the attractive well, respectively. The solid-solid phase transition takes places between two solid phases of the same structure. It is first order and ends at a critical point as the temperature is increased. These are common features with the usual liquid-gas transition. However, two main differences appear neatly. The first one is the strong dependence of the critical point density with the well width parameter δ. The second one is that the critical temperature remains almost invariant in all range of δ. These two features are roughly interchanged in the fluid condensation where the critical density slightly depends on the attractive range while the critical temperature increases with this parameter. We shall discuss below the physical mechanism behind these transitions.

In a recent work, Tejero *et al.*[12] have presented a theoretical study of the phase diagram of systems with extreme pair potentials. Their study includes the solid-solid transition for very short-ranged attractive interactions. They use a different pair potential model for the sake of simplicity in their calculations. However, they have used a *different* theory for the fluid phase and for the solid one. Thus, they lack a consistent description of the full phase diagram. In particular, they cannot ensure the relative stability of the different phases. In this paper we report *consistent* theoretical calculations of the complete phase diagram, including the solid-solid transition, for the square-well potential (2). The rest of the paper is arranged as follows: In Sec. II we summarize our theoretical model and in Sec. III we present and discuss our results, including the comparison with simulation data.

II. THEORY

In this section we summarize the perturbation weighted density approximation (PWDA) which has been recently proposed by us.[13,14] The PWDA has been successfully applied to study the phase diagram of a LJ system.[13] A simplified version, SPWDA, has also been presented and applied to the LJ and Girifalco potentials[14,3] and to a model of colloidal dispersions.[10]

The standard perturbation scheme, successfully used in uniform fluids,[15] provides a density-functional approximation for the Helmholtz free energy, $F[\rho(\mathbf{r})]$, of nonuniform systems. Its general expression is

$$F[\rho(\mathbf{r})] = F_{\rm ref}[\rho(\mathbf{r})] + U_p[\rho(\mathbf{r})]. \tag{3}$$

$F_{\rm ref}$ is the Helmholtz free energy of the reference system and U_p is the contribution to the free energy coming from the attractive perturbation $\varphi_p(r)$. Its explicit form, up to first order, is

$$U_p[\rho(\mathbf{r})] = \frac{1}{2}\int d\mathbf{r}d\mathbf{r}'\rho^{(2)}_{\rm ref}(\mathbf{r},\mathbf{r}')\varphi_p(|\mathbf{r}-\mathbf{r}'|), \tag{4}$$

where $\rho^{(2)}_{\rm ref}(\mathbf{r},\mathbf{r}')$ is, according to first-order perturbation theory, the pair distribution function of the reference system. This function is usually written in terms of $g_{\rm ref}(\mathbf{r},\mathbf{r}')$, the extension of the radial distribution function (RDF) to the case of the inhomogeneous reference system, as

$$\rho^{(2)}_{\rm ref}(\mathbf{r},\mathbf{r}') = \rho(\mathbf{r})\rho(\mathbf{r}')g_{\rm ref}(\mathbf{r},\mathbf{r}'). \tag{5}$$

For uniform phases the density $\rho(\mathbf{r})$ reduces to the mean density and the PWDA recovers the standard perturbation theory. The minimization of the functional with respect to $\rho(\mathbf{r})$ would determine the free energy and the equilibrium structure of the system. However, a previous step is usually needed to use the theory even in the uniform limit; namely, the free energy of the reference system is generally mapped onto that of hard spheres of some effective diameter $d_{\rm HS}$. Thus, some criterion has to be provided to obtain $d_{\rm HS}$ from the reference potential. This is not the case in this work because the natural way to split the potential (2) into reference and perturbation parts already gives a hard sphere system of diameter σ as a reference. The remaining problem is, then, the application to nonuniform phases, like the solid one. Unfortunately, little is known about the RDF in nonuniform systems. Then some additional approximation should be introduced to proceed. The main aim of PWDA theory is to obtain the mapping of the actual $g_{\rm ref}$ into the RDF of the uniform system at some effective density $\hat{\rho}$ which will, in general, depend on the position. This scheme has been successfully used with some very simple prescriptions for $\hat{\rho}(\hat{\rho} = \rho(\mathbf{r}), \rho = [\rho(\mathbf{r}) + \rho(\mathbf{r}')]/2$, etc.) in cases where the nonuniformity is not very strong like, for example, a liquid-vapor interface far above the triple

point.[16,17] However, it is clear that this kind of recipe, based on the local density $\rho(\mathbf{r})$, will not work when the system has a pronounced nonuniformity, like the solid phase. In these cases the local density may reach values many times larger than the close-packing density in the uniform system. The alternative proposed by PWDA theory is based on the exact *local compressibility* equation (see the Appendix in Ref. 13)

$$\int d\mathbf{r}'\rho(\mathbf{r}')[g_{\mathrm{ref}}(\mathbf{r},\mathbf{r}')-1] = -1 + \frac{k_BT}{\rho(\mathbf{r})}\frac{d\rho(\mathbf{r})}{d\mu}, \qquad (6)$$

where μ is the chemical potential. Precisely, $\hat{\rho}$ is defined through Eq. (6) substituting the nonuniform RDF $g_{\mathrm{ref}}(\mathbf{r},\mathbf{r}')$ by its uniform limit $g_{\mathrm{ref}}[|\mathbf{r}-\mathbf{r}'|,\hat{\rho}(\mathbf{r})]$ and solving for $\hat{\rho}(\mathbf{r})$. It has been shown[14] that this prescription *together* with a smooth perturbation $\varphi_p(r)$ at $|\mathbf{r}| \approx |\mathbf{R_1}|$, where $|\mathbf{R_1}|$ is the first-neighbor distance in the solid phase, gives a very accurate result for the perturbation energy in the solid phase. The last condition is achieved if we use the Week-Chandler-Anderson[18] (WCA) criterion to split the intermolecular potential.

The simplified version, SPWDA, is based on the usual compressibility equation[15] which can be obtained from integration of the local compressibility equation (6). In this version, the $g_{\mathrm{ref}}(\mathbf{r},\mathbf{r}')$ is mapped into a RDF of a uniform system, $g_{\mathrm{ref}}(|\mathbf{r}-\mathbf{r}'|,\hat{\rho})$, where the effective density does not depend on position. The SPWDA gives competitive accuracy and significantly reduces the computational effort without adding any approximation with respect to the PWDA. The price paid for it is that it only applies to macroscopically homogeneous systems like the solid phase.[14] Notice that to elucidate the relative stability of the different phases (and, therefore, to obtain the phase diagram) it is important to use a theory with some grade of sophistication. In particular, the theory should be able to describe all the involved phases using the same approximation and, of course, it should be free of parameter adjustment. Our theory is, so far, the only one which satisfies both crucial requisites (see Ref. 14 for a discussion of these points).

III. RESULTS AND DISCUSSION

We have used the SPWDA to determine the phase diagram of the square-well potential. The potential parameters σ and ϵ are used as distance and energy units, respectively. We have studied the evolution of the phase diagram with the parameter δ in the range 0.01–1.00. The lower values correspond to an extremely short-ranged attractive interaction while $\delta \approx 0.3$ would already correspond to the attractive range of the Lennard-Jones potential. In this work we have limited ourselves to study the face-centered-cubic (fcc) structure for the solid phase. This will allow us to compare with simulations. Besides, other possible solid structures, except the hexagonal close packed (hcp), have a much smaller packing density and, therefore, they can be ignored. On the other hand, the free energy difference between fcc and hcp structures is quite small. Figures 1–4 show the results for a selected set of δ values (dotted lines indicate transitions between metastable states and they are included for the sake of comparison).

We shall first describe the general characteristics of these diagrams. For small δ (Fig. 1) the phase diagram exhibits the expanded solid-condensed solid transition which ends at a critical point. The phase diagram shows also a fluid-solid transition and a triple point where the fluid, the expanded solid, and the condensed solid coexist. The fluid condensation, i.e., the gas-liquid transition, does occur but only at very low temperatures and between metastable states. As δ increases (Fig. 2), the solid-solid transition moves towards lower densities but the critical temperature remains practically unchanged. At the same time, the critical temperature of the fluid condensation rises but still this transition takes place between metastable states. For δ higher than 0.06 (Fig. 3) the solid-solid critical point becomes a metastable state with respect to the state of a fluid coexisting with a solid at the same temperature. Therefore the solid-solid transition, between stable states, disappears. The critical temperature of the fluid condensation continues to rise but still remains below the sublimation line. Therefore there is a range for δ values (approximately from 0.06 to 0.25) where the phase diagram only exhibits two stable phases, fluid and solid, and a first-order transition between them (Fig. 3). For $\delta \approx 0.25$ (Fig. 4) the gas-liquid transition emerges above the sublimation line. Then the phase diagram presents the usual pattern of a simple classical system: the three stable phases (gas, liquid, and solid), the three transitions (condensation, sublimation, and melting), the condensation critical point, and the gas-liquid-solid triple point. Notice that for $\delta \approx 0.25$ (Fig. 4), the attractive potential still corresponds to a weak interaction and the stable liquid phase is confined into a very narrow temperature range between the triple and the critical temperatures. For $\delta \approx 0.30$ the phase diagram is very similar to that of the LJ diagram, as it should be.

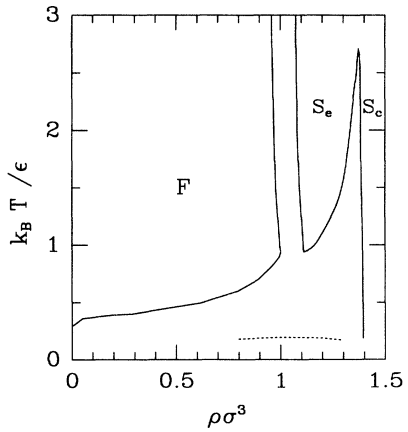

FIG. 1. Phase diagram of the square-well potential in the temperature-density plane for $\delta = 0.01$. Labels F, S_e, and S_c mean fluid, expanded solid, and condensed solid, respectively. The dotted line at the bottom is the first-order transition between the metastable liquid and gas phases.

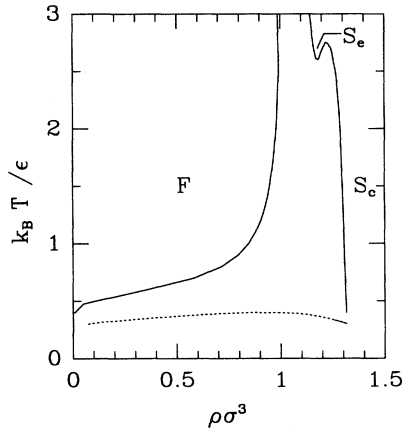

FIG. 2. As in Fig. 1 for $\delta = 0.05$.

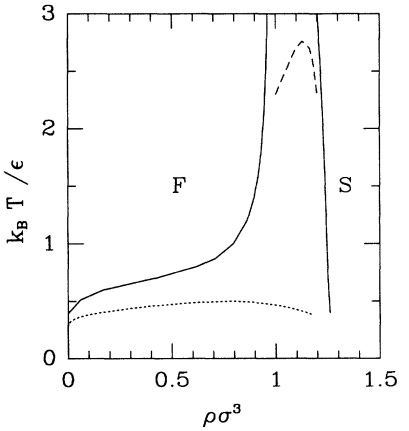

FIG. 3. As in Fig. 1 for $\delta = 0.08$. Label S means solid. The dashed line represents the first-order transition between the metastable expanded and condensed solid phases.

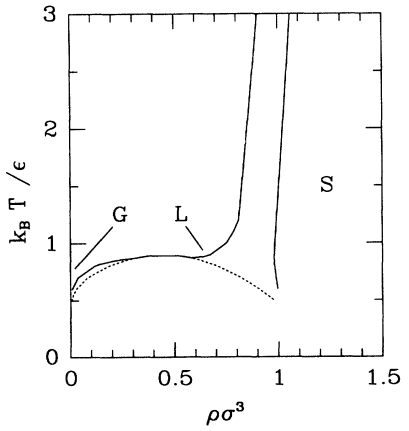

FIG. 4. As in Fig. 1 for $\delta = 0.25$. Labels G, L, and S mean gas, liquid, and solid, respectively.

The qualitative evolution of the solid-solid transition versus δ, discussed above, agrees with the simulation results of Bolhuis and Frenkel.[11] We shall come back to this point later. Our theoretical approach also allows us to determine the complete phase diagram and, in particular, predicts that the fluid condensation is a different transition from the solid condensation (the expanded solid-condensed solid transition). In fact the theory predicts the simultaneous existence of both transitions for small δ values (Figs. 1–3), though the fluid condensation takes place between metastable states. Furthermore, we shall show below that the only common feature of these two transitions is the necessary existence of an attractive interaction, but the mechanisms giving place to them are quite different.

After the above general description of the phase diagrams, we shall now pay attention to several qualitative and important details related to the solid-solid transition:

(1) We have already mentioned that the solid-solid critical temperature is almost invariant with respect to δ while the critical density decreases as δ increases.

(2) The density of the condensed solid which coexists with the expanded solid depends slightly on the temperature (Figs. 1 and 2) while the density of the expanded solid which coexists with the condensed solid decreases significantly with the temperature (Fig. 1).

(3) On the other hand, at a given temperature, this first-order transition becomes stronger — i.e., the density jump increases — as δ increases (see Figs. 1–3). Notice that, despite this fact, the transition disappears at high δ, because the coexisting phases become metastable with respect to the fluid-solid transition.

(4) The fluid-solid transition at high enough temperatures tends to the melting transition of hard spheres, as it should be. In Figs. 1–4 it can be appreciated that the coexistence fluid and solid densities of this transition tend to $\rho = 0.9433$ and $\rho = 1.0609$, respectively, the values predicted by the present theory for the hard sphere melting. The interesting point is that, for high δ, the fluid-solid transition bends towards lower densities as the temperature decreases (Figs. 3 and 4), as is expected. However, for low δ it bends towards higher densities (Figs. 1 and 2). Moreover, this bending towards higher densities ends at the fluid-solid-solid triple point. At temperatures lower than this triple point the fluid coexistence density recovers its expected dependence with temperature.

We shall discuss now the mechanisms giving place to all the above features with the help of our theory. Bolhuis and Frenkel[11] have already given an intuitive argument to explain the solid-solid transition dependence on the parameter δ. Basically, the transition would appear at the density where the nearest neighbors (NN) distance is comparable to the well width δ. Under this condition, each particle significantly reduces its interaction energy. If this reduction outweighs the loss of entropy, the transition takes place. This pure geometrical effect is clearly reflected in the phase diagram and, in fact, the critical density is located at the density where the NN distance of the fcc structure is just $\sigma + \delta$. At high enough temperatures the effect of the entropy cancels any effect of

the attractive interaction; hence the solid-solid transition must end at a critical point. Now we shall complete this argument, in order to describe all other features displayed by the phase diagram, using details of the theoretical calculations.

As is usual, we describe the local density of the solid phase as a sum over all the lattice sites $\mathbf{R}$ of normalized Gaussian peaks,

$$\rho(\mathbf{r}) = C \sum_{\mathbf{R}} e^{-\alpha(\mathbf{r}-\mathbf{R})^2}, \tag{7}$$

where C is a normalization constant. The Gaussian parameter α gives information on the particle localization. A large α value means a strong localization of the particle around its equilibrium position in the solid lattice. At the opposite limit, $\alpha = 0$, expression (7) reduces to the mean density of a fluid. Obviously, in the solid phase, it is expected that α increases with density but decreases with temperature. This is well known and it is illustrated in Fig. 5 for $\delta = 0.05$ where we present theoretical results for α versus solid mean density at several temperatures. Notice that α in Fig. 5 is that one which minimizes the free energy functional (3) at each density and temperature. This does not mean that all of them correspond to stable states. The stability is determined after the coexistence between the different phases is found (by the common tangent method). Thus, for instance, for $k_BT/\epsilon = 2.0$ the α values shown in Fig. 5 at densities below $\rho = 1.25$ correspond to solid states which are metastable with respect to a state where a fluid coexists with a solid at the same temperature (see Fig. 2). For a temperature as low as $T = 5$, the highest shown in Fig. 5, α does not appreciably differ from that of hard spheres over the entire density range. At lower temperatures and low densities the NN distance is larger than $\sigma + \delta$ and, therefore, the equilibrium position of each particle is outside the attractive interaction wells. Under these conditions the Gaussian, representing each particle, tries to broaden itself to feel the attractive well of its neighbors, reducing in this way its interaction energy. This strategy is also favored by the configurational entropy (i.e., the ideal gas free energy). However, the process is not very efficient because the hard core repulsion (free energy excess with respect to the ideal gas) prevents the Gaussian expansion. Figure 6 shows all these contributions to the free energy versus α for a given temperature and density. The total free energy minimum determines the corresponding α for this temperature and density. Observe in this figure that the effect of the attractive energy on the α which minimizes the free energy is quite small. Accordingly Fig. 5 shows no appreciable differences over all densities below the solid-solid critical density even at low temperatures. However, at densities just above the critical density the NN distance is already smaller than, but close to, $\sigma+\delta$. Then, to decrease the energy, the Gaussian tries to confine itself inside the square well. Now the hard core favors the confinement (see Fig. 7), but the configurational entropy is opposed to it. The final balance will always give an α larger than that corresponding to the hard sphere solid at the same density. This is shown also in Fig. 5. If the density is further increased, the Gaussian center moves towards the interior of the well. Moreover, at high densities the hard sphere solid density peaks are already quite narrow. Then, most of the Gaussian is inside the square well and it does not need to confine too much to diminish the energy. This is the origin of the maximum shown in Fig. 5. Finally, at high enough density, close to packing, the strong particle localization makes no difference between the α of the actual system and that of the hard sphere solid, no matter how low the temperature is. This is reflected in Fig. 5 which shows how α tends to the hard sphere value at the high density limit for all temperatures.

The above study on the behavior of α will help us to discuss and understand the four qualitative aspects of the phase diagram mentioned above. We begin with the in-

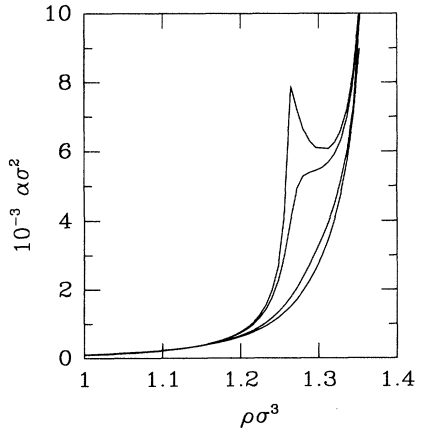

FIG. 5. Solid density parameter α versus mean solid density for $\delta = 0.05$. The temperature changes from $k_BT/\epsilon = 0.5$ (top curve showing a sharp maximum) to 0.6, 2.0, and 5.0 (bottom curve which is indistinguishable from the hard sphere result).

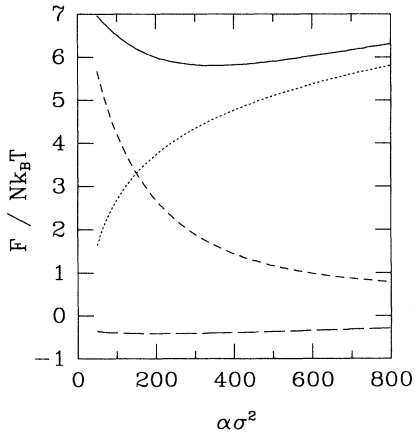

FIG. 6. Contributions to the solid free energy per particle (in k_BT units) versus α for $\delta = 0.03$, $\rho\sigma^3 = 1.15$, and $k_BT/\epsilon = 2.0$. The solid line at the top is the total free energy. The dotted line is the ideal gas contribution. The dashed line is the hard core free energy excess and the long-dashed line at the bottom is the attractive energy.

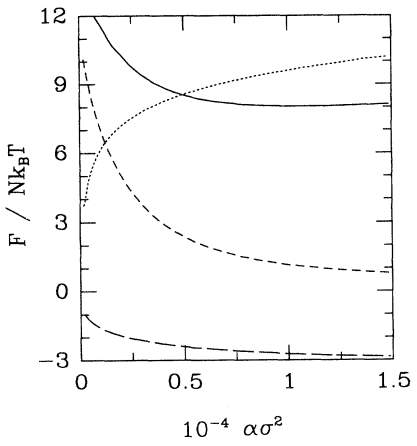

FIG. 7. As in Fig. 6 but for $\rho\sigma^3 = 1.35$.

dependence of the solid-solid critical temperature on the parameter δ [point (1)]. Let us consider the free energy per particle (i.e., per Gaussian) in k_BT units. This is the sum of the temperature-independent hard sphere contribution (ideal gas free energy plus hard core free energy excess) and the attractive energy. The latter is an integral restricted over the square well. At densities lower than the critical one the Gaussian is practically outside the square well. Then the contribution to the free energy is very small. The free energy (Fig. 6) and α (Fig. 5) do not differ too much from those of hard spheres except for low enough temperatures. But just for densities equal or greater than the critical one the Gaussian is essentially inside the well and, then, the attractive energy per particle must be of the order of $-6\epsilon/k_BT$ (as seen in Fig. 7). This free energy depleting when crossing the critical density only depends on temperature; if this is small enough, the free energy will decrease significantly and it will drive the transition. An essential point is that this result does not depend on δ; then the solid-solid critical temperature is expected to be δ independent. In fact, we have found that, over the entire range of δ values, the attractive contribution per particle at the estimated critical point is $F_{\text{att}}/Nk_BT_c = -1.01$ (with an error around 1%). It is then quite appealing to infer that only when the thermal particle energy k_BT is lower than the well depth ϵ is the Gaussian captured in the well and the transition can take place. It is interesting to notice that the attractive energy works in a different way in the liquid-gas condensation. In this case the attractive energy per particle clearly depends on δ. In particular, in a mean field approximation (i.e., approximating g_{ref} by a step function) it is proportional to δ^3, and therefore th critical temperature will increase with δ as is well known in simple classical fluids.

We can now easily understand point (2). Figure 8 shows the solid free energy versus mean density for $\delta = 0.01$ at different temperatures. Notice that, as we have discussed above, the free energy does not change appreciably with temperature for densities below the critical one ($\rho_c = 1.37$). However, above the critical density, i.e., when the equilibrium position of the particles is inside the attractive wells, the free energy suffers a local depletion with the appearance of an elbow (see Fig. 8). When the temperature decreases the elbow size increases, but its position remains practically unchanged. The common tangent method, applied to the free energy curves of Fig. 8, immediately gives the coexistence densities of the condensed and expanded solid phases. Clearly, the coexisting density of the condensed solid is rather attached around the minimum of the elbow, while the coexisting density of the expanded solid moves towards lower densities when the temperature decreases. Figure 1 shows this characteristic asymmetric behavior of the solid-solid coexistence curve. Of course, at high enough temperatures (above the critical one), the elbow is very flat and no common tangent can be drawn in the free energy curve: There is no solid-solid transition.

The coexistence densities of the fluid-solid transition are anchored at high temperatures, practically above $k_BT/\epsilon = 5$, at the coexistence densities of the fluid-solid transition of hard spheres, as it should be. This compels those coexistence densities, at low temperatures, not to be very different from those at high temperatures and to be rather independent of δ, as Figs. 1–4 show [see, however, discussion of point (4) below]. On the other hand, the coexistence densities of the solid-solid transition, as we have discussed, decrease as δ increases (though its difference increases; i.e., the transition is stronger). Therefore, at some δ value, the solid-solid transition is preempted by the fluid-solid transition (see Fig. 3). Thus point (3) is also explained.

Finally we will discuss the last characteristic of the phase diagram [point (4)]. Figures 1 and 2 show that the density domain of stability of the fluid phase increases with respect to that of the hard sphere fluid as the temperature decreases until the fluid-solid-solid triple point is reached. When the temperature is further decreased, below the triple point, the fluid density domain of stability begins to decrease. This can be easily understood in the light of the previous discussions. We have already noticed that the expanded solid hardly detects the attrac-

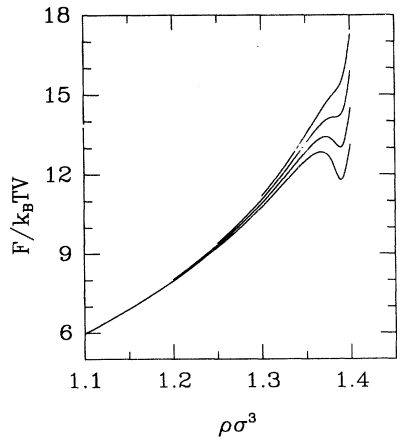

FIG. 8. Free energy density of the solid phase (in k_BT units) versus mean density for $\delta = 0.01$ at $k_BT/\epsilon = 2.0$, 1.5, 1.2, and 1.0 (from top to bottom).

tive square well. However, the fluid particles ($\alpha = 0$) are able to see it at any density. Therefore the fluid is, obviously, much more efficient in reducing its free energy (and hence increasing its stability) than the expanded solid phase. This explains the bending of the fluid-solid transition towards higher densities for temperatures above the triple point. However, for temperatures below the triple point, the fluid must compete with the condensed solid phase. As we have already seen, the NN distance in this phase is smaller than $\sigma + \delta$ and therefore all particles are inside the attractive wells reducing the free energy quite efficiently. Then the density range of fluid stability recedes below the triple point (Fig. 2). For larger values of δ, when all the expanded solid states become metastable (Fig. 3) or when the expanded solid state becomes unstable (Fig. 4), the usual bending of the fluid-solid transition towards lower densities at low temperatures is recovered. Notice that this unusual bending of the fluid-solid transition at low enough δ (around or less than 0.01) gives place to an interesting effect: Starting from a solid phase at low densities and at high temperatures we can arrive at the fluid phase (through a transition) lowering the temperature but keeping the density constant.

Now we compare our results with the computer simulations (Monte Carlo) due to Bolhuis and Frenkel.[11] All the qualitative features of the solid-solid transition in the phase diagram obtained by simulation have been reproduced by the theory. As one could expect from a mean field approach, the estimated critical temperature ($k_B T_c/\epsilon \approx 2.7$) is larger than the simulation result ($k_B T_c/\epsilon \approx 1.7$). However, it is too large, at least if we take into account the corresponding result for the liquid-gas critical temperature where the discrepancy is around 10%. Unfortunately, there are no simulations of the fluid phase for the range of δ where the solid-solid transition is present in the phase diagram. Then an important part of our predictions cannot be compared with simulations. We think that our theoretical predictions would be confirmed in future simulations, at least qualitatively. For example, Fig. 9 shows the critical density of the solid-solid and liquid-gas transitions and the solid-solid-liquid and the solid-liquid-gas triple points. The agreement with the simulations is excellent for the solid-solid transition. The agreement is the expected for the case of the liquid-gas transition at high values of δ.[19,20] It would be very interesting to know if this remains so for low δ values. Our theory predicts the (solid-liquid-gas) triple point for classical fluids in agreement with simulation results; then we expect the same behavior at low δ values for this triple point. We expect a similar agreement also for the solid-solid-fluid triple point. However, obviously, this will fail when the liquid-gas critical temperature is close to the solid-liquid-gas triple temperature (Fig. 4) or when the solid-solid critical temperature is close to the solid-solid-fluid triple temperature (Fig. 2).

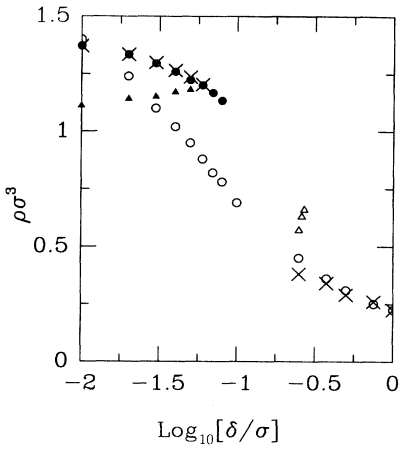

FIG. 9. Critical and triple-point densities versus δ. Solid-solid critical density (solid circles). Liquid-gas critical density (open circles). Expanded solid density at the solid-solid-fluid triple point (solid triangles). Liquid density at the solid-liquid-gas triple point (open triangles). The crosses are the Bolhuis-Frenkel simulation results for the solid-solid transition and the simulation results of Vega *et al.* for the liquid-gas transition.

ACKNOWLEDGMENTS

We would like to thank Dr. E. Velasco for careful reading of the manuscript. This work was supported by the Dirección General de Investigación Científica y Técnica of Spain, under Grant No. PB91-0090.

[1] A. Cheng, M.L. Klein, and C. Caccamo, Phys. Rev. Lett. **71**, 1200 (1993).
[2] M.H.J. Hagen, E.J. Meijer, G.C.A.M. Mooij, D. Frenkel, and H.N.W. Lekkerkerker, Nature (London) **365**, 425 (1993).
[3] L. Mederos and G. Navascués, Phys. Rev. B **50**, 1301 (1994).
[4] L.A. Girifalco, J. Phys. Chem. **96**, 858 (1992).
[5] P.N. Pusey, W.C.K. Poon, S.M. Ilett, and P. Bartlett, J. Phys. Condens. Matter **6**, A29 (1994).
[6] F. Leal Calderon, J. Bibette, and J. Biais, Europhys. Lett. **23**, 653 (1993).
[7] D.H. Napper, *Polymeric Stabilization of Colloidal Dispersions* (Academic, New York, 1983), Chap. 16.
[8] E.J. Meijer and D. Frenkel, Phys. Rev. Lett. **67**, 1110 (1991).
[9] M.H.J. Hagen and D. Frenkel, J. Chem. Phys. **101**, 4093 (1994).
[10] L. Mederos and G. Navascués, J. Chem. Phys. **101**, 9841 (1994).
[11] P. Bolhuis and D. Frenkel, Phys. Rev. Lett. **72**, 2211 (1994).
[12] C.F. Tejero, A. Daanoum, H.N.W. Lekkerkerker, and M. Baus, Phys. Rev. Lett. **73**, 752 (1994).

[13] L. Mederos, G. Navascués, P. Tarazona, and E. Chacón, Phys. Rev. E **47**, 4284 (1993).
[14] L. Mederos, G. Navascués, and P. Tarazona, Phys. Rev. E **49**, 2161 (1994).
[15] J.P. Hansen and I.R. McDonald, *Theory of Simple Liquids* (Academic, New York, 1986).
[16] S. Toxvaerd, Mol. Phys. **26**, 91 (1973).
[17] L. Mederos, E. Chacón, G. Navascués, and M. Lombardero, Mol. Phys. **54**, 211 (1985).
[18] H.C. Andersen, D. Chandler, and J.D. Weeks, Phys. Rev. A **4**, 1918 (1971).
[19] J. Chang and S.I. Sandler, Mol. Phys. **81**, 745 (1994).
[20] L. Vega, E. de Miguel, L.F. Rull, G. Jackson, and I.A. McLure, J. Chem. Phys. **96**, 2296 (1992).